Anti-tissue factor antibody-mediated immuno-SPECT imaging of tissue factor expression in mouse models of pancreatic cancer

AYA SUGYO[1*], WINN AUNG[1*], ATSUSHI B. TSUJI[1], HITOMI SUDO[1], HIROKI TAKASHIMA[2],
MASAHIRO YASUNAGA[2], YASUHIRO MATSUMURA[2],
TSUNEO SAGA[3] and TATSUYA HIGASHI[1]

[1]Department of Molecular Imaging and Theranostics, National Institute of Radiological Sciences,
National Institutes for Quantum and Radiological Science and Technology (QST-NIRS), Inage, Chiba 263-8555;
[2]Division of Developmental Therapeutics, Exploratory Oncology Research and Clinical Trial Center,
National Cancer Center, Kashiwa, Chiba 277-8577; [3]Department of Diagnostic Radiology,
Kyoto University Hospital, Sakyo-ku, Kyoto 606-8507, Japan

Abstract. Tissue factor (TF) has emerged as a critical factor in oncogenic events, leading to the development of TF-targeted diagnostic and therapeutic approaches. A non-invasive imaging method to evaluate target molecule expression with high sensitivity and high quantitative ability is imperative for selecting the appropriate patients for TF-targeted therapy. To elucidate the potential of ^{111}In-labeled anti-TF antibody 1849 ([111]In-1849) as an immuno-single photon emission computed tomography (SPECT) probe targeting TF, we evaluated TF-dependent *in vitro* binding as well as *in vivo* biodistribution and tumor accumulation of [111]In-1849 in pancreatic cancer cells/models with varying TF expression levels. TF expression levels in five human pancreatic cancer cell lines, BxPC-3, BxPC-3-TF-knockout (BxPC-3-TFKO), Capan-1, PSN-1 and SUIT-2, were examined by immunofluorescence. Binding of [111]In-1849 to each cell line was assessed. Biodistribution and imaging studies were also conducted in tumor-bearing mice. Furthermore, the relationship of TF expression with cell binding and tumor uptake was analyzed. In the immunofluorescence studies, BxPC-3 exhibited the highest TF expression, followed by Capan-1, PSN-1, SUIT-2 and BxPC-3-TFKO. Cell binding assays revealed that BxPC-3 cells had the highest [111]In-1849 binding, followed by PSN-1, Capan-1 and SUIT-2; no binding was detected in BxPC-3-TFKO cells. The BxPC-3 xenograft was clearly visualized on [111]In-1849 SPECT/CT, and the highest uptake was detected on day 4. The biodistribution of [111]In-1849 on day 4 revealed that tumor uptake ranged from 8.68 to 50.58% of the injected dose per gram of tissue; BxPC-3 had the highest uptake and SUIT-2 had the lowest. TF expression was significantly associated with cell binding ($R^2=0.79$, P<0.05) and tumor uptake ($R^2=0.92$, P<0.01). The association of [111]In-1849 uptake with TF expression suggests the potential application of non-invasive imaging with radiolabelled 1849 for selecting the appropriate patients who would likely respond to TF-targeted therapies in clinical practice.

Correspondence to: Dr Atsushi B. Tsuji, Department of Molecular Imaging and Theranostics, National Institute of Radiological Sciences, National Institutes for Quantum and Radiological Science and Technology (QST-NIRS), 4-9-1 Anagawa, Inage, Chiba 263-8555, Japan
E-mail: tsuji.atsushi@qst.go.jp

*Contributed equally

Introduction

Molecular-targeted approaches using antibodies have attracted tremendous interest for early diagnosis and new therapeutic options for cancer, such as antibody-drug conjugate (ADC) therapy, radioimmunotherapy (RIT) and photoimmunotherapy (PIT). Molecular imaging techniques with certain monoclonal antibody-based probes are being developed to distinguish tumors from normal tissues by exploiting tumor-specific molecules. Expression levels of the target molecules, however, may differ due to the intrinsic heterogeneity of tumors, even among those derived from similar organs. A better understanding of these characteristics through non-invasive nuclear medicine imaging would facilitate patient selection, improve selection of treatment strategies, and help to predict treatment sensitivity.

Pancreatic cancer is a major life-threatening disease with a 5-year survival rate of 8% for all stages combined (1). It is

predicted to be the second leading cause of cancer-related deaths by 2030 (2). Therefore, there is an urgent need to explore suitable target molecules and their related imaging and therapeutic agents to facilitate early diagnosis and the selection of an effective treatment for pancreatic cancer. Patients with malignancies, including pancreatic cancer, have a higher risk of venous thromboembolism than patients without malignancy (3,4). Cancer coagulopathy is triggered by tissue factor (TF) (5-7). TF is a transmembrane glycoprotein (47-kDa) present on the cell surface that mediates a variety of physiologically and pathophysiologically relevant functions. Its overexpression is associated with thrombogenicity, tumor angiogenesis, cell signaling, tumor cell proliferation and metastasis (7-9). TF is a key element in the initiation of the extrinsic coagulation cascade (10-12). Although TF normally safeguards vascular integrity by inducing hemostasis upon injury, abnormal expression of TF in various tumors is related to the malignant cycle of blood coagulation (13-15). Therefore, the malignant blood coagulation cycle is postulated to generate versatile cancer stroma, leading to cancer invasion into vessels, tumor proliferation, metastasis, hemorrhage, fibrin clot formation and replacement with collagenous tissue (8,9,16,17). A wide variety of malignancies, including pancreatic cancer, exhibit aberrant TF expression (18-20). In addition, high TF expression in pancreatic cancer has been revealed to be correlated with tumor grade, extent, metastasis and invasion, in contrast to normal pancreas with low TF expression (12,19,21,22). Haas *et al* evaluated TF expression in eight human pancreatic cancer cell lines, including BxPC-3, and reported aberrant TF expression at both the RNA and protein levels (5). In parallel with TF expression in the cell lines, they also demonstrated that most of the tissue specimens from pancreatic cancer patients had highly variable TF expression when determined by immunofluorescence staining (5). Furthermore, TF was expressed not only on the tumor cell surface, but also in the tumor stroma (11) and on tumor-associated vascular endothelial cells (23).

TF is a potential target for cancer diagnostic imaging or therapy, and high-affinity anti-TF antibodies have been developed (24). Application of anti-TF monoclonal antibody 1849 (rat IgG$_{2b}$), which reacts with human TF antigen, to ADC demonstrated superior antitumor activity in pancreatic cancer xenograft models (25). In addition, we successfully visualized TF-expressing orthotopic glioma in a mouse xenograft model using an ^{111}In-labeled anti-TF antibody 1849 ([111]In-1849) probe (26). The relationship between tumor uptake of the probe and TF expression levels, however, has not yet been analyzed.

In the present study, we investigated the *in vitro* binding of the [111]In-1849 probe to five pancreatic cancer cell lines, BxPC-3, BxPC-3-TF-knockout (BxPC-3-TFKO), Capan-1, PSN-1 and SUIT-2, which have different TF expression profiles. We also evaluated the *in vivo* uptake of the probe in xenograft tumors derived from these cell lines in biodistribution studies. The relationship of TF expression with cell binding and tumor uptake of [111]In-1849 was evaluated by regression analysis.

Materials and methods

Cells. Human pancreatic cancer cell lines (BxPC-3, Capan-1 and PSN-1) were obtained from the American Type Culture Collection (ATCC; Manassas, VA, USA). SUIT-2 cells were obtained from the Japanese Collection of Research Bioresources Cell Bank (Osaka, Japan) (27). The TF gene of BxPC-3 was disrupted using the CRISR/Cas9 system with a CRISPR plasmid (U6-gRNA/CMV-Cas9-GFP; Sigma-Aldrich; Merck KGaA, Darmstadt, Germany) and Lipofectamine LTX and PLUS reagent (Thermo Fisher Scientific, Inc., Waltham, MA, USA) according to the manufacturer's protocol, and the established cell line was named BxPC-3-TFKO. BxPC-3 and BxPC-3-TFKO were maintained in RPMI-1640 medium (Wako Pure Chemical Industries, Ltd., Osaka, Japan) supplemented with 10% fetal bovine serum (FBS; Sigma-Aldrich; Merck KGaA) in a humidified incubator maintained at 37°C with 5% CO_2. PSN-1 and SUIT-2 were maintained in Dulbecco's modified Eagle's medium (DMEM; Wako Pure Chemical Industries, Ltd.) supplemented with 10% FBS. Capan-1 was maintained in Iscove's modified Dulbecco's medium (IMDM; Wako Pure Chemical Industries, Ltd.) supplemented with 20% FBS.

TF protein expression analysis by immunofluorescence staining. Immunofluorescence staining was conducted as previously described (28,29). Briefly, cells were grown on glass coverslips and fixed in cold methanol for 5 min. Non-specific binding was blocked by applying Block Ace reagent (Dainippon Pharmaceutical Co., Ltd., Osaka, Japan) with 10% goat serum for 30 min at room temperature. Cells were incubated with anti-TF antibody 1849 (rat IgG$_{2b}$) (26,30) as a primary antibody overnight at 4°C. A secondary anti-rat antibody conjugated with Cy3 (diluted 1:1,000; cat. no. 109-165-003; Jackson ImmunoResearch Laboratories, West Grove, PA, USA) was applied for 30 min at room temperature. Nuclei were stained with 4',6-diamidino-2-phenylindole (DAPI) in mounting medium (Vector Laboratories, Inc., Burlingame, CA, USA). Images were obtained with an exposure time of 0.017 sec for detecting TF using a fluorescence microscope (Olympus Corp., Tokyo, Japan). Signal intensities of fifteen cells of each cell line's image were measured using ImageJ software (ver. 1.46r; NIH; National Institutes of Health, Bethesda, MD, USA). The mean ± SD value was used as an index of TF protein expression.

Radiolabeling of the antibody. To label the single-photon emission computed tomography (SPECT) tracer ^{111}In-labeled anti-TF antibody 1849 ([111]In-1849), the antibody was first conjugated with a chelating agent, *p*-SCN-Bn-CHX-A''-DTPA (DTPA) (Macrocyclics, Inc., Dallas, TX, USA) as previously described (31). The DTPA-conjugated antibody was purified using a Sephadex G-50 (GE Healthcare, Little Chalfont, UK) column (centrifuged once at 700 x g for 2 min). The conjugation ratio of DTPA to the antibody was estimated to be ~1.5 based on cellulose acetate electrophoresis. Typically, the DTPA-conjugated antibody (50 µg) was mixed with 1.48 MBq of indium-111 chloride ([111]InCl$_3$; Nihon Medi-Physics, Tokyo, Japan) in 0.5 M acetate buffer (pH 6.0) and the mixture was incubated for 30 min at room temperature. The radiolabeled antibody was separated from free ^{111}In using a Sephadex G-50 column (centrifuged at 700 x g for 2 min). The labeling yield of [111]In-1849 ranged from 82.4 to 85.8%, the radiochemical purity was 100%, and the specific activity was 24.2-25.4 kBq/µg.

In vitro binding assay. Cell binding of five cell lines (BxPC-3, BxPC-3-TFKO, Capan-1, PSN-1 and SUIT-2) was examined as previously described (32). Briefly, in the cell binding assay, 3-4 days after seeding, the cells were detached and cell suspensions prepared ($1.0x10^7$, $5.0x10^6$, $2.6x10^6$, $1.3x10^6$, $6.3x10^5$, $3.1x10^5$, $1.6x10^5$, $7.8x10^4$ and $3.9x10^4$) in phosphate-buffered saline (PBS) with 1% bovine serum albumin (BSA; Sigma-Aldrich; Merck KGaA). The suspension was incubated with [111]In-1849 on ice for 60 min. After washing, the radioactivity bound to cells was assessed with a gamma counter (ARC-370; Aloka Medical, Ltd., Tokyo, Japan). The association between cell binding at $5x10^6$ cells and TF expression was evaluated by simple regression analysis using GraphPad Prism 6 (GraphPad Software, Inc., La Jolla, CA, USA).

Subcutaneous tumor mouse model. The animal experimental protocol was approved by the Animal Care and Use Committee of the National Institute of Radiological Sciences (Chiba, Japan), and all animal experiments were conducted in accordance with the Guidelines Regarding Animal Care and Handling of the National Institute of Radiological Sciences. Thirty BALB/cA Jcl-nu/nu male mice (5 weeks old, 18-20 g; CLEA Japan, Inc., Tokyo, Japan) were maintained under specific pathogen-free conditions. Mice (6 mice/each model) were subcutaneously inoculated in the left shoulder with BxPC-3 ($4x10^6$), BxPC-3-TFKO ($1x10^6$), Capan-1 ($1x10^6$), PSN-1 ($1x10^6$) and SUIT-2 ($1x10^6$) cells under isoflurane anesthesia. Animals were maintained at controlled temperature (23±3°C) and humidity (50±20%) under a 12/12-h light/dark cycle. Animals were provided food and water *ad libitum*. We employed mice in which subcutaneous tumors reached a diameter of ~9 mm.

In vivo SPECT/CT imaging with [111]In-1849. For SPECT imaging, a mouse (n=1/tumor model) was injected with ~1.85 MBq of [111]In-1849 into a tail vein. The injected protein dose was adjusted to 50 µg/mouse by adding the intact antibody. At 1, 2, 3 and 4 day(s) after the injection, the mice were anesthetized by isoflurane inhalation and imaged using a VECTor/CT SPECT/CT Pre-Clinical Imaging system with a multi-pinhole collimator (MILabs, Utrecht, The Netherlands). SPECT data were acquired for 15 min on day 1, 20 min on day 2, 25 min on day 3, and 30 min on day 4 after injection, taking into account the half-life of In-111. SPECT images were reconstructed using a pixel-based ordered-subsets expectation maximization algorithm with eight subsets and two iterations on a 0.8-mm voxel grid without attenuation correction. Computed tomography data were acquired with an X-ray source set at 60 kVp and 615 µA after SPECT scan and images were reconstructed using a filtered back-projection algorithm for cone beam. Merged images were obtained using PMOD software (ver. 3.6; PMOD Technologies GmbH, Zürich, Switzerland). The region of interest was manually drawn over tumors and tracer uptake was quantified as the percentage of injected dose per gram of tissue (%ID/g) using the PMOD software.

Biodistribution of [111]In-1849. When subcutaneous tumors reached a diameter of ~10 mm, the mice (n=5/tumor model) were intravenously injected with 37 kBq of [111]In-1849. The total injected protein dose was adjusted to 50 µg/mouse by adding the intact antibody. Biodistribution experiments for [111]In-1849
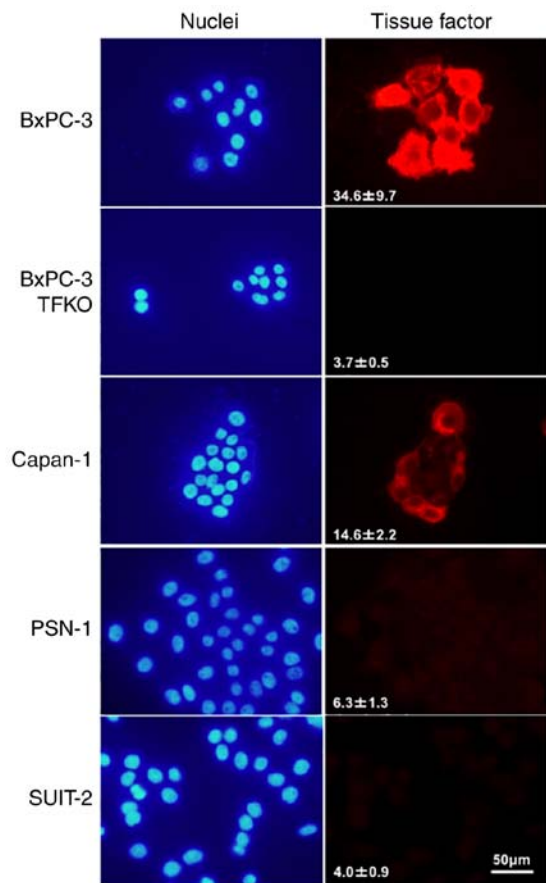

Figure 1. TF protein expression analysis of pancreatic cancer cells, BxPC-3, BxPC-3-TFKO, Capan-1, PSN-1 and SUIT-2. TF protein expression was determined based on the mean fluorescence signal intensities of five cells from each cell line after immunofluorescence staining with the anti-TF antibody (red, right panels). Signal intensity of TF staining (arbitrary unit) is displayed in the right panels. DAPI stained nuclei (blue, left panels). Scale bar, 50 µm. TF, tissue factor; BxPC-3-TFKO, BxPC-3-TF-knockout; DAPI, 4',6-diamidino-2-phenylindole.

were conducted on day 4 after the injection because the largest difference in tumor uptake of [111]In-1849 was observed on day 4 in the immuno-SPECT imaging studies. Five mice for each tumor model were sacrificed by isoflurane inhalation and blood was obtained from the heart. Tumors and organs of interest (blood, brain, heart, lung, liver, spleen, pancreas, stomach, intestine, kidney, muscle and bone) were removed and weighed, and radioactivity counts were measured using the gamma counter. The data were expressed as %ID/g normalized to a 20-g body weight mouse. Tumor uptake data were analyzed by two-way repeated-measures ANOVA, followed by Student-Newman-Keuls (SNK) test. The association between tumor uptake and TF expression was evaluated by simple regression analysis using GraphPad Prism 6 (GraphPad Software, Inc).

Results

TF protein expression in pancreatic cancer cells. TF protein expression levels in five human pancreatic cancer cell lines (BxPC-3, BxPC-3-TFKO, Capan-1, PSN-1 and SUIT-2) were determined by measuring the signal intensities of the cells visualized by immunofluorescence. BxPC-3 had the highest expression, followed by Capan-1, PSN-1, SUIT-2 and BxPC-3-TFKO (Fig. 1).
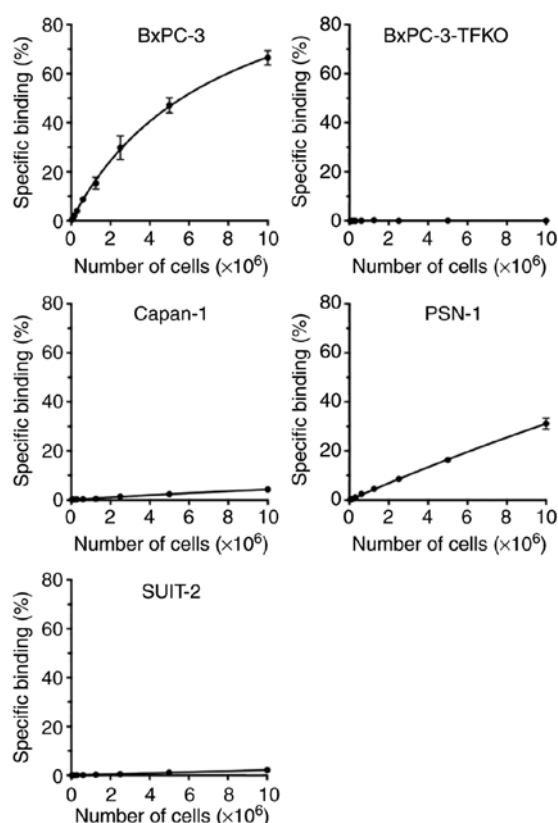
Figure 2. Cell binding assay using [111]In-1849 on pancreatic cancer cells, BxPC-3, BxPC-3-TFKO, Capan-1, PSN-1 and SUIT-2. [111]In-1849, ^{111}In-labeled anti-TF antibody 1849; BxPC-3-TFKO, BxPC-3-TF-knockout.
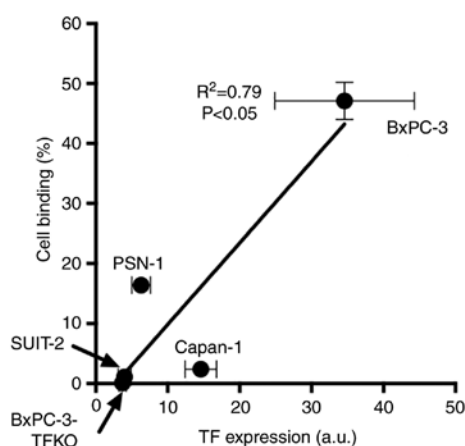

Figure 3. Regression analysis of [111]In-1849 cell binding at $5x10^6$ cells with TF protein expression. a.u., arbitrary unit; TF, tissue factor; [111]In-1849, ^{111}In-labeled anti-TF antibody 1849.
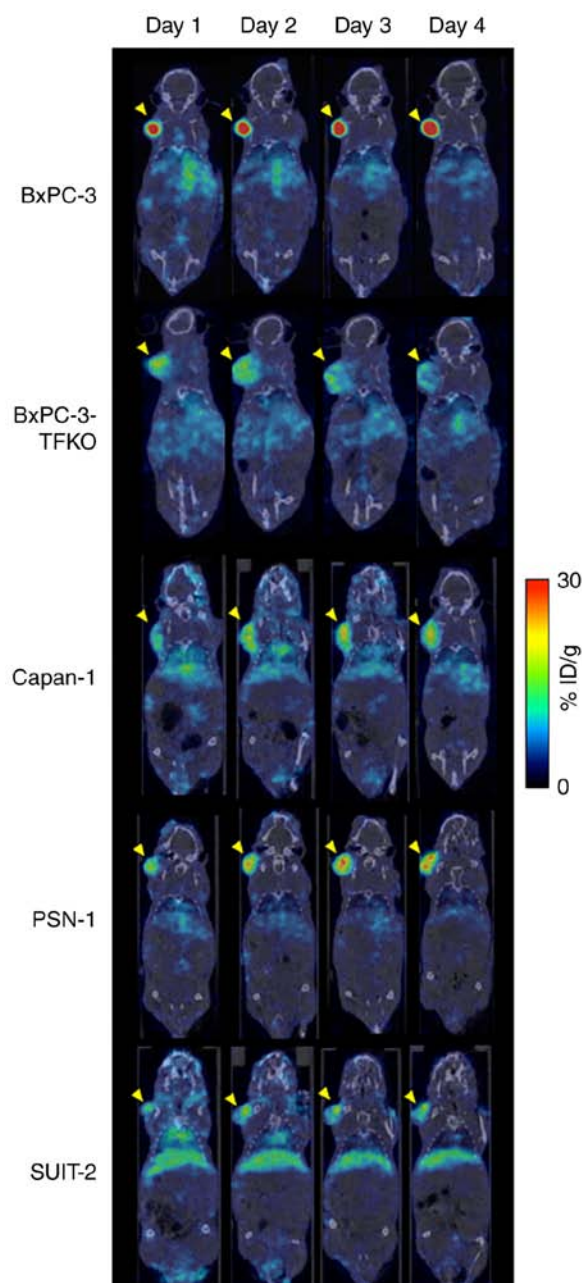

Figure 4. Serial SPECT/CT imaging with [111]In-1849. Representative coronal SPECT/CT images of nude mice bearing BxPC-3, BxPC-3-TFKO, Capan-1, PSN-1 and SUIT-2 xenograft tumors on 1, 2, 3 and 4 days after intravenous injection of 1.85 MBq of [111]In-1849. Yellow arrowheads indicate tumors. [111]In-1849, ^{111}In-labeled anti-TF antibody 1849; SPECT/CT, single-photon emission computed tomography/computed tomography; BxPC-3-TFKO, BxPC-3-TF-knockout.

Cell binding of ^{111}In-labeled anti-TF antibody 1849. Of the five cell lines, [111]In-1849 had the highest binding to BxPC-3 cells, followed by PSN-1, Capan-1 and SUIT-2 (Fig. 2). No cell binding was observed in BxPC-3-TFKO cells (Fig. 2). TF protein expression was significantly associated with the cell binding when cell preparations seeded at $5x10^6$ cells were used for the regression analysis ($R^2=0.79$, $P<0.05$; Fig. 3).

SPECT/CT imaging with [111]In-1849 in tumor-bearing mice. SPECT/CT images in subcutaneous tumor mouse models

bearing BxPC-3, BxPC-3-TFKO, Capan-1, PSN-1 and SUIT-2 tumors were obtained on days 1, 2, 3 and 4 after injection of [111]In-1849. On day 1, high BxPC-3 tumor uptake of 24.9%ID/g was observed and thereafter the uptake increased with time, whereas the background activity continued to decrease, resulting in increased contrast of BxPC-3 tumors over time (Fig. 4). On day 4, BxPC-3 tumor uptake was highest (62.3%ID/g) and PSN-1 tumor uptake was second highest (18.1%ID/g), followed by Capan-1 (15.2%ID/g), SUIT-2 (9.1%ID/g) and BxPC-3-TFKO tumor (9.1%ID/g; Fig. 4). Tumor uptake in PSN-1 and Capan-1 increased with

Table I. Biodistribution of [111]In-1849 in mice bearing pancreatic cancer tumors on day 4.

	BxPC-3	BxPC-3-TFKO	Capan-1	PSN-1	SUIT-2
Blood	10.12±2.67	12.48±1.99	13.95±1.89	10.68±4.56	11.86±2.44
Brain	0.33±0.08	0.36±0.15	0.39±0.14	0.31±0.13	0.40±0.12
Heart	3.29±0.65	3.37±0.62	3.74±0.56	2.83±0.88	3.30±0.79
Lung	4.96±1.07	5.10±1.35	6.39±0.86	4.54±1.62	5.19±1.07
Liver	6.30±0.87	6.99±0.77	6.42±0.80	5.87±0.32	7.85±1.89
Spleen	6.07±2.29	5.39±2.29	7.04±0.76	5.70±2.08	5.92±1.58
Pancreas	1.35±0.29	1.26±0.28	1.85±0.20[a]	1.27±0.46	1.39±0.30
Stomach	1.31±0.30	1.44±0.28	1.75±0.37	1.19±0.39	1.40±0.22
Intestine	1.68±0.47	1.69±0.30	2.05±0.14	1.51±0.57	1.60±0.38
Kidney	4.17±0.95	3.89±0.64	4.55±0.57	3.28±1.10	3.74±0.46
Muscle	0.91±0.23	0.80±0.17	1.06±0.17	0.83±0.26	0.87±0.17
Bone	2.85±0.89	2.33±0.74	3.44±0.48	2.42±1.11	2.54±0.64
Tumor	50.58±14.26	10.59±4.15[b]	25.26±1.84[b]	24.05±4.86[b]	8.68±0.52[b]

Data are expressed as %ID/g ± SD (n=5). [a]$P<0.05$, [b]$P<0.01$ (vs. BxPC-3-bearing mice). [111]In-1849, ^{111}In-labeled anti-TF antibody 1849.
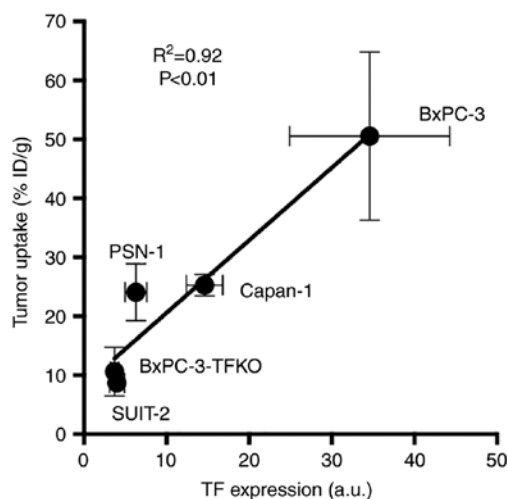

Figure 5. Regression analysis of [111]In-1849 tumor uptake on day 4 with TF protein expression. The a.u. means arbitrary unit. TF, tissue factor; [111]In-1849, ^{111}In-labeled anti-TF antibody 1849.

time like BxPC-3, whereas that of BxPC-3-TFKO and SUIT-2 decreased with time (Fig. 4).

In vivo biodistribution of [111]In-1849. Biodistribution experiments for [111]In-1849 were conducted in nude mice bearing xenograft tumors on day 4 after injection. Tumor uptake of [111]In-1849 was 50.58±14.26%ID/g in BxPC-3, 10.59±4.15%ID/g in BxPC-3-TFKO, 25.26±1.84%ID/g in Capan-1, 24.05±4.86%ID/g in PSN-1, and 8.68±0.52%ID/g in SUIT-2 tumors (Table I). BxPC-3 tumor uptake was significantly higher than that of the others ($P<0.01$; Table I). In all mice, the uptake of [111]In-1849 in the major normal organs, including the liver and kidney, was relatively low (Table I). TF protein expression was significantly associated with the tumor uptake ($R^2=0.92$, $P<0.01$; Fig. 5).

Discussion

Specific probes targeting specific molecules or genetic abnormalities are highly desired for improving the diagnostic and treatment efficiency of pancreatic cancer, which has a dismal clinical outcome. Generally, to visualize cancer with a targeted molecular imaging approach, tumor-specific targets with sufficient expression are important for distinguishing lesions from the surrounding environment, and antibodies are favorable candidates due to their excellent specific binding affinity with compatible antigens and slow rate of disassociation.

The present study aimed to evaluate whether tumor uptake of our monoclonal antibody-based single-photon emission computed tomography (SPECT) probe [111]In-1849 could reflect differences in the tissue factor (TF) expression levels in certain pancreatic cancer models. Various expression levels of TF have been detected in several human pancreatic cancer cell lines (5). In the present study, the TF expression profiles of five human pancreatic cancer cell lines [BxPC-3, BxPC-3-TF-knockout (BxPC-3-TFKO), Capan-1, PSN-1 and SUIT-2] were analyzed by immunofluorescence examination. In good agreement with previous studies, BxPC-3 had the highest signal intensity indicating the highest TF expression among the five cell lines, followed by Capan-1, PSN-1, SUIT-2 and BxPC-3-TFKO (Fig. 1). These cell lines are considered suitable for the purposes of the present study. The cell binding of ^{111}In-labeled anti-TF antibody 1849 ([111]In-1849) to each cell line (Fig. 2) related to the TF expression measured from the signal intensities of cells visualized by immunofluorescence (Fig. 3).

SPECT/CT studies in tumor-bearing mice were conducted to evaluate the temporal change in [111]In-1849 uptake and to determine the temporal kinetics of the biodistribution. The largest difference in tumor uptake was observed on day 4. Therefore, the biodistribution studies were conducted at that time-point. In the biodistribution studies, tumor uptake ranged from 8.68 to 50.58% ID/g; BxPC-3 had the highest

uptake and SUIT-2 the lowest (Table I). TF protein expression was significantly associated with the tumor uptake (Fig. 5). Moreover, the biodistribution studies revealed that [111]In-1849 uptake in the surrounding normal organs, including the liver, spleen and kidneys, which are the major organs involved in the elimination of the probe, and the pancreas, was relatively low (Table I). Therefore, the pharmacokinetics of [111]In-1849 produced minimal background, providing a high-contrast image of tumors with [111]In-1849 in mice bearing pancreatic cancer xenografts.

Higher TF-expressing cancer tissue may be more accessible to administered [111]In-1849 than lower TF-expressing tumors. The present findings suggest that [111]In-1849 will be an excellent probe for non-invasive imaging of TF-expression. [111]In-1849 accumulates in tumors with TF expression based on both active and passive targeting. BxPC-3-TFKO tumors exhibited a little accumulation of [111]In-1849, probably due to passive enhanced permeability and retention in tumors (33).

We previously proposed TF as an alternative potential target for the diagnosis and treatment of cancer. The Alexa Fluor®-647-labeled anti-TF antibody 1849 probe was used for fluorescence imaging in a pancreatic cancer xenograft model (24), and the [111]In-1849 probe for immuno-SPECT imaging in a glioma model (26). Hong *et al* developed a radiotracer, ^{64}Cu-labeled chimeric anti-human TF monoclonal antibody, for immuno-positron emission tomography (PET) imaging of *in vivo* TF expression in pancreatic cancer models (34). PET has higher sensitivity (10^{-11}-10^{-12} mole/l) than SPECT (10^{-10}-10^{-11} mole/l) (35). A gamma-emitting radio-nuclide such as ^{111}In for immuno-SPECT is easier to obtain than a positron-emitting radionuclide, such as ^{64}Cu or [89]Zr for PET because ^{111}In is widely used in routine clinical nuclear medicine practice. The higher sensitivity of PET allows for the detection of smaller tumors compared with SPECT (36), whereas SPECT provides sufficient quality images to interpret disease in routine use and can be more easily conducted in clinics. Both SPECT and PET have potential application in many clinical situations, and further clinical studies are needed to clarify the role of [111]In-1849 immuno-SPECT in clinical oncology imaging.

Some research groups (19,22) evaluated the correlations between the expression of TF and clinicopathologic characteristics. Nitori *et al* reported that TF expression is a useful prognostic marker in pancreatic cancer patients, and that the identification of molecules that could predict a poor prognosis is critical for selecting patients who would benefit from radical treatment or molecular targeting therapy (22). Mainly immunohistochemical examination of tumor tissue sections has been performed to assess target expression. The technique is limited to measuring the expression in a whole tumor region, however, due to biopsy-associated pitfalls and the requirement of multiple invasive procedures. Moreover, target expression may change over time as a result of tumor growth and therapy and thus differ between primary lesions and metastatic foci, and these variabilities are difficult to capture utilizing techniques other than non-invasive imaging. Nuclear medicine imaging using target-specific and sensitive probes offers accurate and real-time measurement of protein expression in a whole tumor because the imaging is sensitive for quantitative assessment of heterogeneous expression and spatiotemporal variance in target expression. Therefore, our radiolabeled anti-TF antibody 1849 has potential utility as a novel probe for predicting which patients are most likely to respond to TF-targeted therapeutic approaches.

TF-targeted therapeutic approaches can be applied to antibody-drug conjugate (ADC) therapy, radioimmunotherapy (RIT) and photoimmunotherapy (PIT). Active targeting of a specific antibody to tumor antigens would enhance the delivery of anticancer candidates (drugs, radionuclides and photosensitizers) to tumor tissues and promote the therapeutic effect. We as well as other groups have reported the usefulness of anti-TF monoclonal antibody in cancer therapy (25,37,38). The anticancer effect of TF-specific ADCs comprising anti-TF antibodies linked to the cytotoxic agent mono-methyl auristatin E was demonstrated in pancreatic tumor xenografts (25) and a broad range of solid tumors xenograft models (37). In contrast, RIT using an antibody labeled with a suitable radionuclide that emits β- or α-radiation to produce cytotoxic effects in target cells is increasingly used for internal radiotherapy (39); Wang *et al* labeled the anti-TF antibody with a β-emitter yttrium-90 and reported its radiothera-peutic effect on human xenograft non-small cell lung cancer tumors in nude mice (38). PIT is also an advanced alternative molecular-targeted cancer therapy exerting highly selective cancer cell death after systemic administration of a photosen-sitizer-conjugated antibody targeting tumor-associated innate antigens and subsequent exposure of light with an appropriate wavelength. We recently investigated the photoimmunothera-peutic effect induced by anti-TF antibody 1849 conjugated to a photosensitizer, indocyanine green, in a TF-expressing BxPC-3 pancreatic cancer model (40). TF-targeted therapies such as ADC, RIT and PIT have desirable prospects, and patient selection for these therapeutic options may be based on TF expression. Our immuno-SPECT imaging helps to reliably visualize and even quantify the expression of the target molecule TF in a non-invasive and repeatable manner. This could ultimately be translated to clinical use, and would enable physicians to make more informed decisions regarding treatment options, patient entry and follow-up. Although the potential utility of [111]In-1849 as a novel probe in preclinical studies was demonstrated, some modifications, such as the development of a humanized form of the antibody, are desir-able to facilitate adoption of this imaging technique and its success in clinical use.

The present study has some limitations: Only one mouse per tumor model was used for SPECT imaging. The clinical effect of anti-TF antibody 1849 on normal tissue could not be accurately assessed since 1849 does not recognize murine TF. Associations between [111]In-1849 uptake and histopatho-logical characteristics or neoplastic tumor grade were not evaluated. Further studies are required to resolve these issues.

In summary, this proof-of-concept study with *in vitro* and *in vivo* experiments demonstrated that immuno-SPECT using ^{111}In-labeled anti-TF antibody 1849 could become a unique imaging modality for non-invasive visualization of the TF expression profile in pancreatic cancer. This novel imaging strategy will likely have an important role in the diagnosis and selection of therapeutic strategies for personalized therapy in the clinic.

Acknowledgements

Availability of data and materials

All data generated or analyzed during this study are included in this published article.

Authors' contributions

WA, ABT, TS and TH were involved in the conception and design of the study. AS, ABT and HS performed the experiments; AS, ABT and HS analyzed the data; WA, ABT, TS and TH interpreted data; HT, MY and YM provided the anti-TF antibody; AS, WA and MY drafted and wrote the manuscript; ABT, HT, YM, TS and TH reviewed and edited the manuscript. All authors read and approved the manuscript and agree to be accountable for all aspects of the research in ensuring that the accuracy or integrity of any part of the work are appropriately investigated and resolved.

Ethics approval and consent to participate

The animal experimental protocol was approved by the Animal Care and Use Committee of the National Institute of Radiological Sciences (Chiba, Japan), and all animal experiments were conducted in accordance with the Guidelines Regarding Animal Care and Handling of the National Institute of Radiological Sciences.

Patient consent for publication

Not applicable.

Competing interests

The authors declare that they have no competing interests.

References

1. Siegel RL, Miller KD and Jemal A: Cancer statistics, 2018. CA Cancer J Clin 68: 7-30, 2018.
2. Rahib L, Smith BD, Aizenberg R, Rosenzweig AB, Fleshman JM and Matrisian LM: Projecting cancer incidence and deaths to 2030: The unexpected burden of thyroid, liver, and pancreas cancers in the United States. Cancer Res 74: 2913-2921, 2014.
3. Stein PD, Beemath A, Meyers FA, Skaf E, Sanchez J and Olson RE: Incidence of venous thromboembolism in patients hospitalized with cancer. Am J Med 119: 60-68, 2006.
4. Woei-A-Jin FJ, Tesselaar ME, Garcia Rodriguez P, Romijn FP, Bertina RM and Osanto S: Tissue factor-bearing microparticles and CA19.9: Two players in pancreatic cancer-associated thrombosis? Br J Cancer 115: 332-338, 2016.
5. Haas SL, Jesnowski R, Steiner M, Hummel F, Ringel J, Burstein C, Nizze H, Liebe S and Löhr JM: Expression of tissue factor in pancreatic adenocarcinoma is associated with activation of coagulation. World J Gastroenterol 12: 4843-4849, 2006.
6. Steffel J, Luscher TF and Tanner FC: Tissue factor in cardiovascular diseases: Molecular mechanisms and clinical implications. Circulation 113: 722-731, 2006.
7. van den Berg YW, Osanto S, Reitsma PH and Versteeg HH: The relationship between tissue factor and cancer progression: Insights from bench and bedside. Blood 119: 924-932, 2012.
8. Leppert U and Eisenreich A: The role of tissue factor isoforms in cancer biology. Int J Cancer 137: 497-503, 2015.
9. Kasthuri RS, Taubman MB and Mackman N: Role of tissue factor in cancer. J Clin Oncol 27: 4834-4838, 2009.
10. Drake TA, Morrissey JH and Edgington TS: Selective cellular expression of tissue factor in human-tissues-implications for disorders of hemostasis and thrombosis. Am J Pathol 134: 1087-1097, 1989.
11. Vrana JA, Stang MT, Grande JP and Getz MJ: Expression of tissue factor in tumor stroma correlates with progression to invasive human breast cancer: Paracrine regulation by carcinoma cell-derived members of the transforming growth factor beta family. Cancer Res 56: 5063-5070, 1996.
12. Khorana AA, Ahrendt SA, Ryan CK, Francis CW, Hruban RH, Hu YC, Hostetter G, Harvey J and Taubman MB: Tissue factor expression, angiogenesis, and thrombosis in pancreatic cancer. Clin Cancer Res 13: 2870-2875, 2007.
13. Matsumura Y, Kimura M, Yamamoto T and Maeda H: Involvement of the kinin-generating cascade in enhanced vascular permeability in tumor tissue. Jpn J Cancer Res 79: 1327-1334, 1988.
14. Fernandez PM, Patierno SR and Rickles FR: Tissue factor and fibrin in tumor angiogenesis. Semin Thromb Hemost 30: 31-44, 2004.
15. Dvorak HF: Tumors: Wounds that do not heal. Similarities between tumor stroma generation and wound healing. N Engl J Med 315: 1650-1659, 1986.
16. Hisada Y, Yasunaga M, Hanaoka S, Saijou S, Sugino T, Tsuji A, Saga T, Tsumoto K, Manabe S, Kuroda J, et al: Discovery of an uncovered region in fibrin clots and its clinical significance. Sci Rep 3: 2604, 2013.
17. Saito Y, Hashimoto Y, Kuroda J, Yasunaga M, Koga Y, Takahashi A and Matsumura Y: The inhibition of pancreatic cancer invasion-metastasis cascade in both cellular signal and blood coagulation cascade of tissue factor by its neutralisation antibody. Eur J Cancer 47: 2230-2239, 2011.
18. Ueda C, Hirohata Y, Kihara Y, Nakamura H, Abe S, Akahane K, Okamoto K, Itoh H and Otsuki M: Pancreatic cancer complicated by disseminated intravascular coagulation associated with production of tissue factor. J Gastroenterol 36: 848-850, 2001.
19. Kakkar AK, Lemoine NR, Scully MF, Tebbutt S and Williamson RC: Tissue factor expression correlates with histological grade in human pancreatic cancer. Br J Surg 82: 1101-1104, 1995.
20. Callander NS, Varki N and Rao LV: Immunohistochemical identification of tissue factor in solid tumors. Cancer 70: 1194-1201, 1992.
21. Hobbs JE, Zakarija A, Cundiff DL, Doll JA, Hymen E, Cornwell M, Crawford SE, Liu N, Signaevsky M and Soff GA: Alternatively spliced human tissue factor promotes tumor growth and angiogenesis in a pancreatic cancer tumor model. Thromb Res 120 (Suppl 2): S13-S21, 2007.
22. Nitori N, Ino Y, Nakanishi Y, Yamada T, Honda K, Yanagihara K, Kosuge T, Kanai Y, Kitajima M and Hirohashi S: Prognostic significance of tissue factor in pancreatic ductal adenocarcinoma. Clin Cancer Res 11: 2531-2539, 2005.
23. Contrino J, Hair G, Kreutzer DL and Rickles FR: In situ detection of tissue factor in vascular endothelial cells: Correlation with the malignant phenotype of human breast disease. Nat Med 2: 209-215, 1996.
24. Tsumura R, Sato R, Furuya F, Koga Y, Yamamoto Y, Fujiwara Y, Yasunaga M and Matsumura Y: Feasibility study of the Fab fragment of a monoclonal antibody against tissue factor as a diagnostic tool. Int J Oncol 47: 2107-2114, 2015.
25. Koga Y, Manabe S, Aihara Y, Sato R, Tsumura R, Iwafuji H, Furuya F, Fuchigami H, Fujiwara Y, Hisada Y, et al: Antitumor effect of antitissue factor antibody-MMAE conjugate in human pancreatic tumor xenografts. Int J Cancer 137: 1457-1466, 2015.

26. Takashima H, Tsuji AB, Saga T, Yasunaga M, Koga Y, Kuroda JI, Yano S, Kuratsu JI and Matsumura Y: Molecular imaging using an anti-human tissue factor monoclonal antibody in an orthotopic glioma xenograft model. Sci Rep 7: 12341, 2017.

27. Iwamura T, Katsuki T and Ide K: Establishment and characterization of a human pancreatic cancer cell line (SUIT-2) producing carcinoembryonic antigen and carbohydrate antigen 19-9. Jpn J Cancer Res 78: 54-62, 1987.

28. Sogawa C, Tsuji AB, Sudo H, Sugyo A, Yoshida C, Odaka K, Uehara T, Arano Y, Koizumi M and Saga T: C-kit-targeted imaging of gastrointestinal stromal tumor using radiolabeled anti-c-kit monoclonal antibody in a mouse tumor model. Nucl Med Biol 37: 179-187, 2010.

29. Sudo H, Tsuji AB, Sugyo A, Ogawa Y, Sagara M and Saga T: ZDHHC8 knockdown enhances radiosensitivity and suppresses tumor growth in a mesothelioma mouse model. Cancer Sci 103: 203-209, 2012.

30. Sugaya A, Hyodo I, Koga Y, Yamamoto Y, Takashima H, Sato R, Tsumura R, Furuya F, Yasunaga M, Harada M, *et al*: Utility of epirubicin-incorporating micelles tagged with anti-tissue factor antibody clone with no anticoagulant effect. Cancer Sci 107: 335-340, 2016.

31. Yoshida C, Tsuji AB, Sudo H, Sugyo A, Kikuchi T, Koizumi M, Arano Y and Saga T: Therapeutic efficacy of c-kit-targeted radioimmunotherapy using 90Y-labeled anti-c-kit antibodies in a mouse model of small cell lung cancer. PLoS One 8: e59248, 2013.

32. Sugyo A, Tsuji AB, Sudo H, Nagatsu K, Koizumi M, Ukai Y, Kurosawa G, Zhang MR, Kurosawa Y and Saga T: Evaluation of 89Zr-labeled human anti-CD147 monoclonal antibody as a positron emission tomography probe in a mouse model of pancreatic cancer. PLoS One 8: e61230, 2013.

33. Matsumura Y and Maeda H: A new concept for macromolecular therapeutics in cancer chemotherapy: Mechanism of tumoritropic accumulation of proteins and the antitumor agent smancs. Cancer Res 46: 6387-6392, 1986.

34. Hong H, Zhang Y, Nayak TR, Engle JW, Wong HC, Liu B, Barnhart TE and Cai W: Immuno-PET of tissue factor in pancreatic cancer. J Nucl Med 53: 1748-1754, 2012.

35. Massoud TF and Gambhir SS: Molecular imaging in living subjects: Seeing fundamental biological processes in a new light. Genes Dev 17: 545-580, 2003.

36. Gnanasegaran G and Ballinger JR: Molecular imaging agents for SPECT (and SPECT/CT). Eur J Nucl Med Mol Imaging 41 (Suppl 1): S26-S35, 2014.

37. Breij EC, de Goeij BE, Verploegen S, Schuurhuis DH, Amirkhosravi A, Francis J, Miller VB, Houtkamp M, Bleeker WK, Satijn D, *et al*: An antibody-drug conjugate that targets tissue factor exhibits potent therapeutic activity against a broad range of solid tumors. Cancer Res 74: 1214-1226, 2014.

38. Wang B, Berger M, Masters G, Albone E, Yang Q, Sheedy J, Kirksey Y, Grimm L, Wang B, Singleton J and Soltis D: Radiotherapy of human xenograft NSCLC tumors in nude mice with a 90Y-labeled anti-tissue factor antibody. Cancer Biother Radiopharm 20: 300-309, 2005.

39. Jain M, Gupta S, Kaur S, Ponnusamy MP and Batra SK: Emerging trends for radioimmunotherapy in solid tumors. Cancer Biother Radiopharm 28: 639-650, 2013.

40. Aung W, Tsuji AB, Sugyo A, Takashima H, Yasunaga M, Matsumura Y and Higashi T: Near-infrared photoimmunotherapy of pancreatic cancer using an indocyanine green-labeled anti-tissue factor antibody. World J Gastroenterol 24: 5491-5504, 2018.